Vacuum 84 (2010) 940–946

Contents lists available at ScienceDirect

Vacuum

journal homepage: www.elsevier.com/locate/vacuum

Optical emission spectroscopy study for nitrogen–acetylene–argon and nitrogen–acetylene–helium 100 kHz and dc discharges

P. Jamroz, W. Zyrnicki*

Chemistry Department, Wroclaw University of Technology, Wyb. Wyspianskiego 27, 50-370 Wroclaw, Poland

ARTICLE INFO

Article history:
Received 27 March 2009
Received in revised form
12 December 2009
Accepted 24 December 2009

Keywords:
Plasma diagnostics
Optical emission spectroscopy
Acetylene–nitrogen
PACVD

ABSTRACT

The optical emission spectroscopy was applied to investigate the middle frequency (100 kHz) and dc low pressure discharges, generated in the nitrogen–acetylene–argon and nitrogen–acetylene–helium mixtures, commonly used for deposits of carbon nitride thin layers. Changes in the emission intensities of the selected species: CN, CH, C, H, N_2, N_2^+ as well as Ar, Ar^+ and He, were studied as a function of the discharge current. Excitation processes occurring in the presence of argon and helium were compared and discussed. The N_2–C_2H_2–Ar and N_2–C_2H_2–He plasmas generated in the 100 kHz and dc glow discharges were characterized by the excitation (Ar, He, H), vibrational (CN, N_2) and rotational (CN, N_2^+) temperatures. A significant deviation from the equilibrium state was observed for the plasma containing argon as well as helium.

1. Introduction

The study of hydrocarbon–nitrogen mixtures with and without noble gases (argon, helium, neon, xenon, krypton) and low pressure discharges is of great importance due to their wide application in production of carbon nitride materials [1–10]. Usually, for the deposition of carbon nitride thin layers (CN:H) by the plasma-assisted chemical vapour deposition (PACVD) method, methane–nitrogen [2,6,7] or acetylene–nitrogen [1,8,9] mixtures at various molecular gas ratios were applied. The quality and properties of the carbon nitride coatings strongly depended on the deposition conditions [9]. It was reported [11,12] that an addition of the noble gases to the hydrocarbon–nitrogen plasma changed the microstructure of the carbon nitride thin layers and, consequently, their properties.

In order to understand the mechanism leading to the formation of materials with relevant parameters, it is necessary to investigate plasma parameters and phenomena which occur in the plasma phase. The reaction occurring in the gas plasma phase as well as concentrations of active species play a key role in the processes leading to the formation of thin layers.

The optical emission spectroscopy (OES), due to its non-invasive character was often applied to investigating and controlling plasma processes [13–15]. It yields information about the excited species in the plasma, the plasma processes as well as the plasma temperatures [13–18]. The optical emission spectroscopy was often employed to investigate the reactive plasma system enabling to the formation of coatings and films [7,17,19]. However, knowledge on plasma characteristics for the system containing acetylene, nitrogen and noble gases is very scarce [20,21]. The interaction of noble gases (Ar, He, Ne, Xe, Kr) plasmas with carbon nitride coatings was investigated by Durrant et al. [20] by means of OES. They recorded and identified species present in plasma spectrum and found that low concentration of CH was produced as a result of an interaction of noble gases with CN:H materials. The optical actinometry techniques, based on the emission intensity measurements, were also applied to the study of acetylene–nitrogen–helium radio frequency plasma [21]. Sung et al. [12] showed that an addition of argon to the acetylene – nitrogen microwave plasma significantly enhanced the emission intensity of CN radical. Dinescu et al. [22] studied a low pressure arc generated in the acetylene–nitrogen–argon mixture by the OES technique to know mechanism of chemical reactions.

Previously [16], we investigated the middle frequency (100 kHz) and direct current (dc) plasmas generated in the nitrogen–acetylene mixtures, using OES and the optical actinometry technique. Here, the effect of the addition of noble gases (Ar or He) to the nitrogen–acetylene 100 kHz and dc plasma was analyzed versus the discharge current. The plasma parameters, i.e. electron "excitation", vibrational and rotational temperatures were determined and compared for dc and the 100 kHz plasma.

2. Experimental setup

The experimental setup was described in the earlier works [16,19]. Briefly, the middle frequency (100 kHz) or direct current

* Corresponding author. Tel./fax: +48 71 3202494.
E-mail address: wieslaw.zyrnicki@pwr.wroc.pl (W. Zyrnicki).

0042-207X/$ – see front matter © 2010 Elsevier Ltd. All rights reserved.
doi:10.1016/j.vacuum.2009.12.019

(dc) discharge was generated between two parallel Armco steel electrodes (diameter 22 mm, thickness 2 mm, space between the electrodes 16 mm) in a Pyrex glass chamber. The plasma reactor contained the quartz window enabling observation of the plasma radiation between the electrodes. The reactor walls were cooled by tap water. The JY Triax 320 monochromator (resolution 0.05 nm in the first order for diffraction grating with 1200 grooves mm^{-1}) and the PGS-2 spectrograph (resolution 0.012 nm for diffraction grating with 651 grooves mm^{-1}) working with photomultipliers (Hamamatsu R-928 or DH-3), were applied here to record spectra. The changes of all optical system sensitivities versus the wavelength (from 200 to 800 nm) were corrected by means of the CL2 Bentham Reference Lamp. The UV achromatic lens ($f = 80$) were used to focus the plasma radiation on the entrance slit of the spectrometer or the spectrograph. The radiation of plasma was collected near the cathode in the negative glow region.

The gas mixtures flowing through the glass chamber were pumped continuously using the rotational pump with the cryogenic trap (liquid nitrogen). The pressure gauge (Pfeiffer PKR 251) was applied here to control the chamber pressure. During all the experiments, the pressure was maintained at 6 Torr (800 Pa). The gases used, i.e.: acetylene, nitrogen, argon and helium, were 99.99% grade pure. The N_2:C_2H_2:Ar(He) ratio was 1:1:1 for each measurement.

The current was varied in the range from 60 to 120 mA for the dc and 100 kHz discharges. The operating powers of both discharges were the same. The current increase in the discharges from 60 to 120 mA caused the growth of the voltage from 500 V to 700 V and from 700 V to 985 V for the N_2–C_2H_2–Ar and N_2–C_2H_2–He mixtures, respectively.

3. Results and discussion

3.1. Emission intensities of species in the N_2–C_2H_2–Ar and N_2–C_2H_2–He mixtures

The emission spectra of 100 kHz and dc discharges in the argon–nitrogen–acetylene and nitrogen–acetylene–helium mixtures were measured in the range of wavelength from 200 to 800 nm. The main species observed in the N_2–C_2H_2–Ar and N_2–C_2H_2–He discharges were: N_2^+, N_2, CN, H, CH, NH and C. The same species were noted in the acetylene–nitrogen plasma [19]. Additionally, in the mixture containing argon numerous Ar I lines with the excitation energy from 13 to 15.5 eV and Ar II lines (excitation energies 19–22 eV, total excitation energies from 35 to 38 eV) were detected. When, helium was introduced, instead of argon, to the acetylene–nitrogen plasma several atomic lines of He I were observed. The most intensive lines of He I were noted at 388.86; 447.15; 501.57; 587.56 and 667.81 nm. The He I line at 388.86 nm was partially overlapped by the (0–0) band of N_2^+ with the band head at 391.44 nm. No ionized helium lines could be recorded, due to high ionization energy of helium (24.58 eV). Intensities of Ar I and ArII lines were considerably higher in the 100 kHz plasma in comparison to those in the dc plasma. A similar effect was observed for He I lines, which were more intensive in the 100 kHz discharge. Generally, the increase of current caused the growth of emission intensities of Ar I, Ar II and He I in the N_2–C_2H_2–Ar and N_2–C_2H_2–He mixtures, respectively. Emission spectra of the N_2–C_2H_2–Ar and N_2–C_2H_2–He plasma were compared in Fig. 1.

The following species: CH, CN, C, H, N_2^+ and N_2, may play an important role in the plasma processes leading to the formation of carbon nitride materials and thus the emission intensities of these species were monitored versus the discharge current. The lines and molecular bands of the species as well as their spectroscopic data were presented in the Table 1.

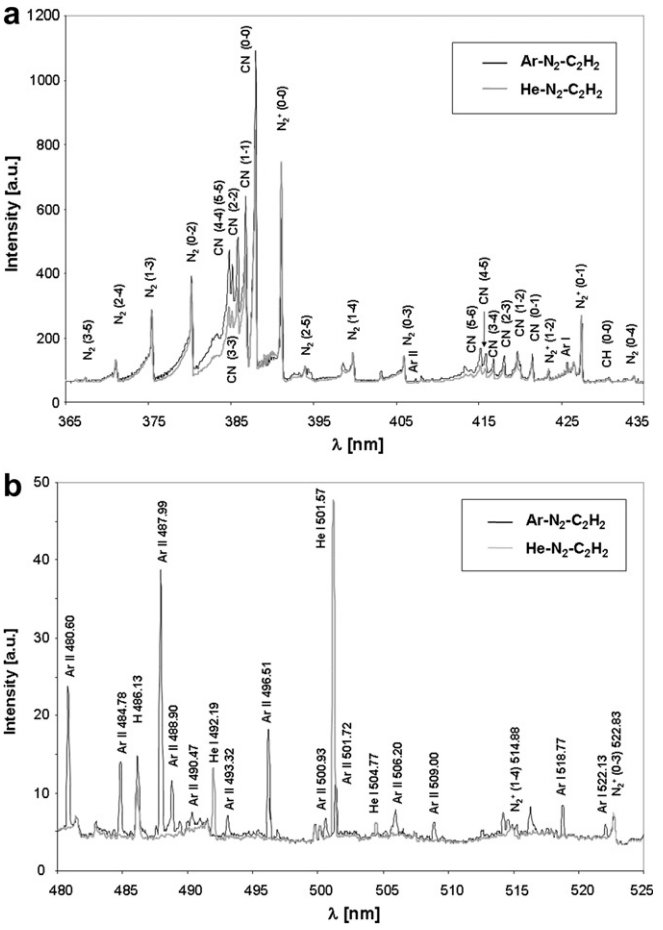

Fig. 1. The emission spectra of the N_2–C_2H_2–Ar and N_2–C_2H_2–He mixtures in the region a) from 365 to 435 nm and b) from 480 to 525 nm.

The variations of the emission intensities of H, CH, CN and C versus the discharge current are shown in Figs. 2 and 3 for the 100 kHz and dc plasmas. The change of the current from 60 to 120 mA led to an increase in the intensities of H, CH, CN and C in the both analyzed mixtures and discharges. In the 100 kHz as well as dc discharges, the intensities of H, CH and CN radicals were higher than in the case of the N_2–C_2H_2–Ar mixture.

Cracking the C–H bond in the acetylene (H–C≡C–H) molecule by the electron impact is probably a first fragmentation step, because the energy of the C≡C bond (10 eV) is higher than the energy of the C–H bond (5.8 eV) in acetylene [22].

$$C_2H_2 + e = C_2H + H + e \quad (1)$$

The C_2H radical may be then dissociated to the CH molecule and the H atom as a result of impact with argon ions [23]. On the other hand, the metastable states of argon with the energies of 11.55 eV Ar($^3P_2$) and 11.72 eV Ar($^3P_0$) in the N_2–C_2H_2–Ar mixture may also contribute

Table 1
List of the investigated species.

Species	Wavelength [nm]	Transition	Threshold energy [eV]
H	656.28	$3d^2$ ($D_{3/2}$)–$2p^2P^o_{3/2}$	12.1
C	247.86	$3s^1$ (P^o)–$2p^2$ (^1S)	7.68
CH	431.44	(0–0) $A^2\Delta$–$X^2\Pi$	2.9; ~ 11
CN	388.43	(0–0) $B^2\Sigma$–$X^2\Sigma$	3.2
N_2	380.49	(0–2) $C^3\Pi_u$–$B^3\Pi_g$	11.2
N_2^+	391.44	(0–0) $B^2\Sigma^+{}_u$–$X^2\Sigma^+{}_g$	3.1; 18.7

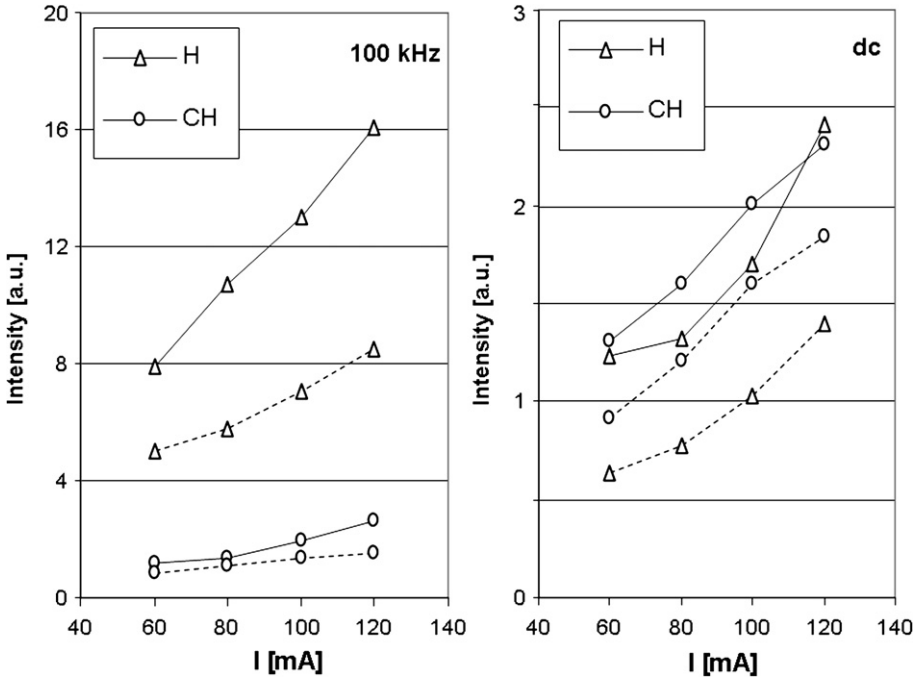

Fig. 2. The emission intensities of H and CH versus the discharge current in the N_2–C_2H_2–Ar (solid line) and N_2–C_2H_2–He (broken line) mixtures.

in the dissociation processes of acetylene and/or products originating from acetylene [20,23]. It can be the reason why the CH and H intensities were higher in the argon than in the helium atmosphere.

Fig. 4 illustrates the N_2^+ and N_2 emission intensities in the N_2–C_2H_2–Ar and N_2–C_2H_2–He dc and 100kHz discharges. Generally, the increase of the discharge current resulted in the growth of intensities of the N_2^+ and N_2 molecules. Only the intensity of N_2 in the N_2–C_2H_2–He dc plasma slightly decreased versus the discharge current. The introduction of argon, instead of helium, to the nitrogen -acetylene 100 kHz plasma did not cause any significant changes in the emission of N_2. No similar effect was noticed for the dc plasma, where the N_2 emission intensity in the N_2–C_2H_2–Ar mixture was higher than in the N_2–C_2H_2–He mixture. In the both analyzed discharges, significantly higher emission intensities of N_2^+ (Fig. 4) were observed in the mixture containing helium, in comparison to the plasma with argon. The ionization degree of molecular nitrogen, deduced from the ionic molecule to neutral molecule intensity ratio was also higher in the presence of helium.

The experimental results for N_2^+ can be explained by the contribution of He. Helium, probably in the metastable excited state, contributed in the production mechanism of N_2^+. It was reported that the excited state of $N_2^+(B)$ may be populated by the interaction of nitrogen with metastable states of helium, i.e. He ($^3S_1$) and/or He ($^1S_0$), as a result of Penning ionization process [13]:

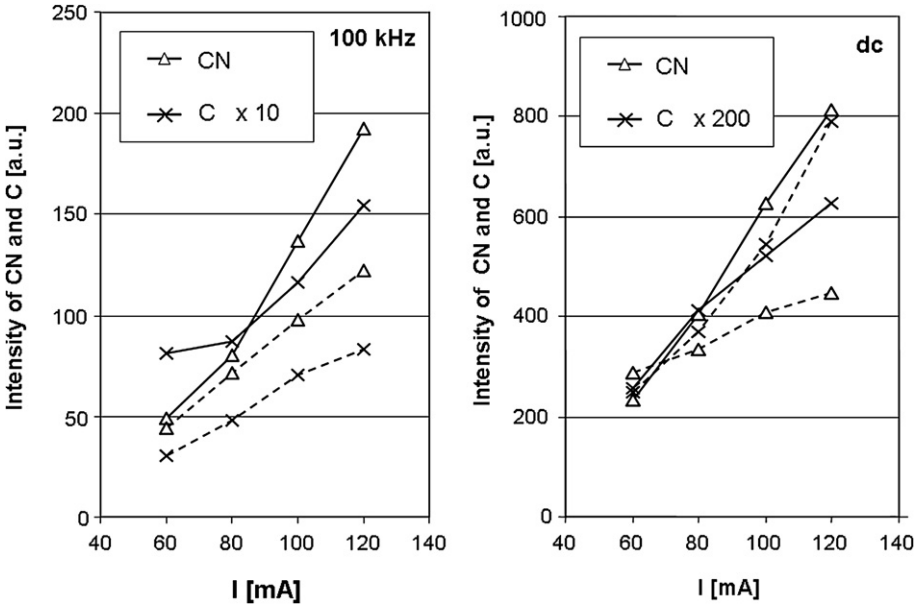

Fig. 3. The effect of argon (solid line) and helium (broken line) in the nitrogen–acetylene mixture on the emission intensities of CN (Δ) and C (×).

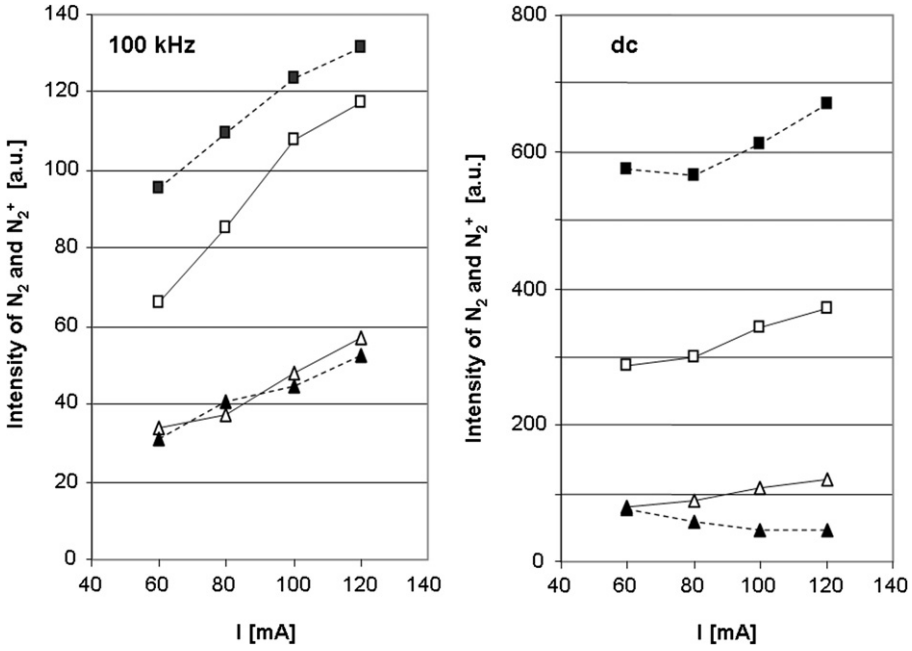

Fig. 4. The emission intensities of N_2^+ and N_2 for the 100 kHz and dc plasmas in the N_2–C_2H_2–Ar (solid line) and N_2–C_2H_2–He (broken line) mixtures.

$$N_2(X) + He^m = N_2^+(B) + He + e \quad (2)$$

Thus, the addition of helium to the nitrogen–acetylene mixture increased the emission intensity of $N_2^+(B)$ as well as ionization rate of nitrogen.

Both CN and CH species identified in the plasma play a significant role in the formation of CN:H coatings [24]. The IR results of deposited materials from acetylene–nitrogen plasma revealed the formation of CN and CH bonds in coatings [9,21]. Moreover, Perreira et al. [24] found a good correlation between emission of CN and CH species and IR signal of bonds (CN, CH) in the CN:H materials.

3.2. Plasma temperatures

In order to describe the energy distributions and phenomena in plasma, the dc and 100 kHz low pressure discharges were characterized by means of the electron "excitation", as well as vibrational and rotational temperatures. The plasma generated in low pressure discharge is usually not in the thermodynamic equilibrium state [16]. Several temperatures (translation, rotational, vibrational, excitation, etc.) can be distinguished. A simultaneous determination of these temperatures enables wide characteristics of plasma and the evaluation of the equilibrium phenomena [19].

The excitation temperatures of the atomic argon T_{exc}(Ar) and helium T_{exc}(He) were calculated with the use of the Boltzmann plot method, employing the relation:

$$\ln\left(\frac{I_{em}^{nm}\lambda_{nm}}{g_n A_{nm}}\right) = C - \frac{E_n}{kT_{exc}} \quad (3)$$

where: I – is the emission intensity of line, λ – wavelength, g – statistical weight, A – transition probability, E – energy of the upper level, k – Boltzmann constant, C – constant, n, m indexes of upper and lower states, respectively

Plotting the $\ln(I_{em}\lambda/gA)$ versus the energy of the upper levels (E_n) yields the straight line with the slope equal to $-1/kT_{exc}$. Ten atomic lines of Ar (at 675.28; 687.13; 696.54; 703.03; 706.72; 714.70; 720.70; 727.29; 737.21; 751.47 nm) and five atomic lines of He (at 282.91; 447.15; 471.32; 501.57; 504.77 nm) were selected here for temperature determination.

The excitation temperature of hydrogen T_{exc}(H) was computed using the so called two line method [14]:

$$\frac{I_1}{I_2} = \left(\frac{g_1 A_1 \lambda_2}{g_2 A_2 \lambda_1}\right)\exp\left(-\frac{E_1 - E_2}{kT_{exc}}\right) \quad (4)$$

Two strong atomic lines of hydrogen, i.e. H_α at 656.56 nm and H_β at 486.13 nm were applied. The spectroscopic constants of the Ar I, He I and H lines were taken from NIST Atomic Spectra Database [25].

The vibrational temperatures (T_{vib}) of N_2, CN were calculated using the Boltzmann plot method from the relation [14]:

$$\ln\left(\frac{I_{v'v''}}{q_{v'v''}\nu_{v'v''}^4}\right) = C - \frac{G(v')}{kT_{vib}} \quad (5)$$

where: I – is the emission intensity of the vibrational band measured at the head, q – Franck–Condon factor, ν – the transition frequency, $G(v')$ – the vibrational energy of the upper state.

Four bands of $B^2\Sigma^+$–$X^2\Sigma^+$ of the CN molecule, i.e. (0–0), (1–1), (2–2), (3–3), six bands of N_2, i.e. (0–2); (1–3); (2–4); (1–0); (2–1); (3–2) were employed.

The rotational temperatures (T_{rot}) were determined using the rotational lines of (0–0) band of $B^2\Sigma^+$–$X^2\Sigma^+$ of CN and the (0–0) band of $B^2\Sigma_u^+$–$X^2\Sigma_g^+$ of N_2^+ by means of the expression [14]:

$$\ln\left(\frac{I_{K'K''}}{K' + K'' + 1}\right) = C - \frac{F(K')}{kT_{rot}} \quad (6)$$

where: I – is the emission intensity of the rotational line, $F(K')$ – the energy of the upper rotational state, K' and K'' – the rotational quantum numbers of the upper and lower states, respectively.

The rotational spectra of CN (0–0) and N_2^+ (0–0) bands (see in Fig. 5) were measured in the fifth order by the high-resolution spectrometer (resolution 0.0024 nm). The rotational lines of the R – branch of N_2^+ (from R_8 to R_{21}) and rotational lines of P – branch of CN (from P_1 to P_{18}) were selected here for the measurements of the N_2^+ and CN rotational temperature, respectively. The overlapping of

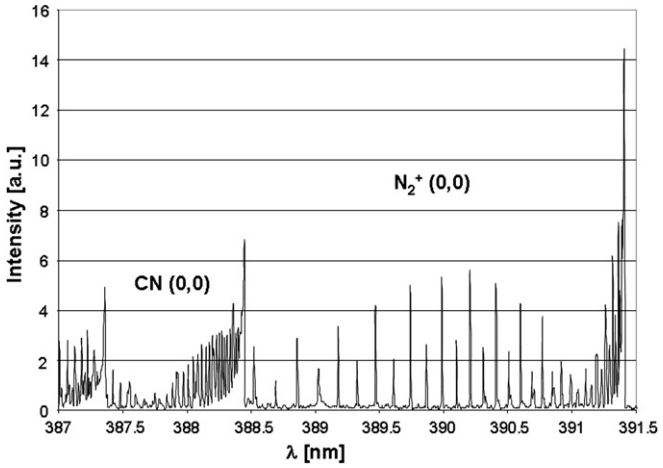

Fig. 5. The high-resolution spectra of CN (0–0) and N_2^+ (0–0).

the P-rotational lines of CN band and overlapping of He I line with R-rotational lines of N_2^+ were taken into account. The other details on the determination of excitation, vibrational and rotational temperatures as well as molecular constants were presented in the previous articles [14,19].

The distribution of the analyzed excitation atomic, vibrational and rotational populations of species was found to follow the Boltzmann law. The obtained temperatures were shown in Figs. 5, 6 and 7. The standard deviation uncertainties of the temperature values were: 15–20%, ~15% and 2–5%, respectively for the excitation, vibrational and rotational temperatures.

Changes in the excitation temperatures of Ar I, H and He I in the N_2–C_2H_2–Ar and N_2–C_2H_2–He mixtures were presented in the Fig. 6 for the 100 kHz and dc plasmas. The excitation temperature of Ar I and He I slightly increased with the current of discharge. In the N_2–C_2H_2–Ar mixture, the highest temperature was observed for Ar I (12,000–14,500 K), while the excitation temperature of H was slightly lower: 9500–10,100 K and 9000–10,300 K for the 100 kHz and dc discharges, respectively. The excitation temperature of He I varied from 3000 K to 3600 K and from 3200 K to 3600 K for the 100 kHz and dc plasmas, respectively. The comparable values of the excitation temperature of He I (3000–3800 K) were reported in the various type of helium plasmas [26]. In the case of the N_2–C_2H_2–He mixture, the excitation temperature of H was significantly higher than T_{exc}(He) and changed from 10000 K to 13000 K in both analyzed plasmas.

The vibrational temperatures of CN and N_2 were demonstrated in Fig. 7. The CN vibrational temperature was about two times higher than the N_2 vibrational temperature. The addition of Ar, instead of He, to the N_2–C_2H_2 mixture resulted in a growth in the T_{vib}(CN) by about 500 K and 1000 K, in the 100 kHz and dc plasma, respectively. At the same conditions, the vibrational temperatures of N_2 were equal 2600–2700 K and 2600–3200 K and were practically independent from the gas mixture composition as well as the current.

The rotational temperatures of CN and N_2^+ were collected in the Fig. 8. As can be observed in the Fig. 8 the CN and N_2^+ rotational temperatures, measured at the same current, were consistent for the dc and 10 kHz discharges, independently of the working gas composition. The rotational temperatures increased versus the current and varied in the range from 640 K to 820 K and from 770 K to 920 K for the N_2–C_2H_2–He and N_2–C_2H_2–Ar mixtures, respectively. The growth of rotational temperature versus current in examined mixtures is due to increase of the discharge power. The lower value of the rotational temperature of N_2^+ (440 K) was noted Kutasi et al. [27] in the dc nitrogen plasma.

The introduction of argon, instead of helium, to the nitrogen–acetylene mixture resulted in an increase in the rotational temperature by about ~120 K in the both examined discharges. A similar effect was also observed by Shimada et al. [28] in the argon and helium low pressure inductively coupled plasma.

The rotational temperatures determined from different species, i.e. N_2^+ and CN were consisted, both in the dc and 100 kHz discharges. The experimental results for the rotational temperatures of CN and N_2^+ indicated that rotational–translational relaxation were sufficiently fast to equilibrate translational (gas) and rotational temperatures and thus the rotational temperature represented here the translation/gas temperature.

The measurements of the rotational temperature and the electrode surface temperature were published for the nitrogen and nitrogen-hydrogen atmospheres and at similar conditions by

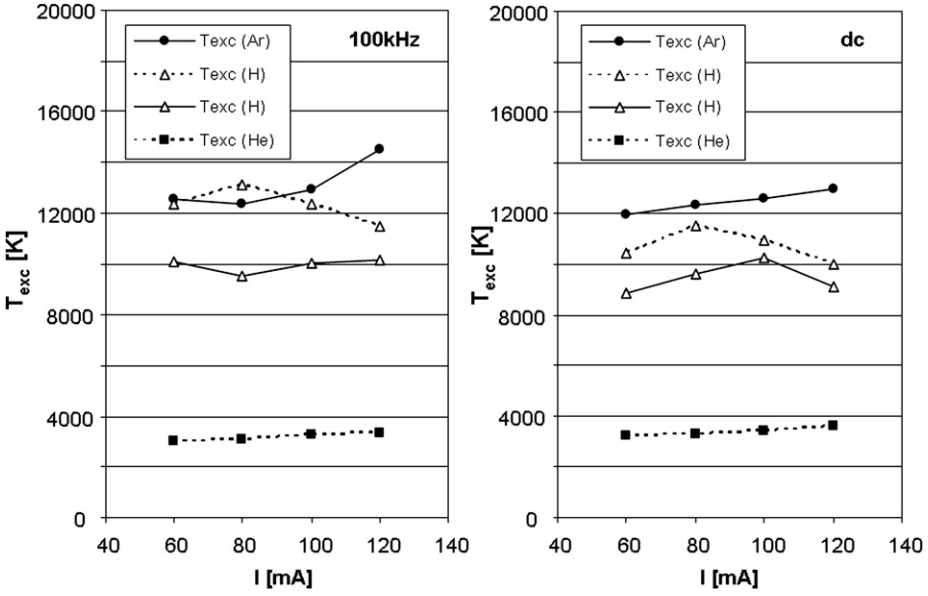

Fig. 6. The excitation temperatures of Ar, He and H versus the discharge current in the mixture containing argon (solid line) and helium (broken line).

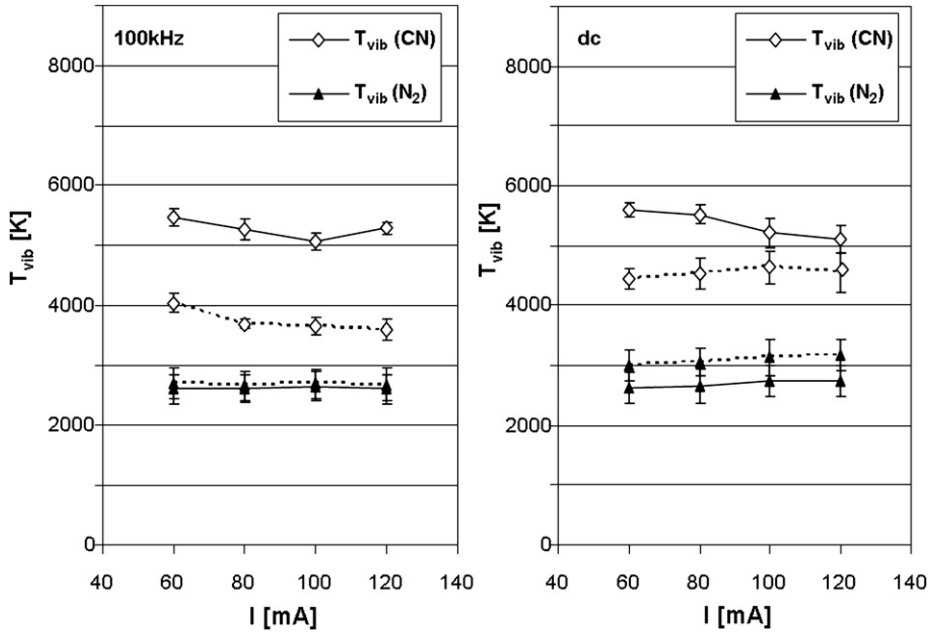

Fig. 7. The vibrational temperatures of CN and N_2 in the N_2–C_2H_2–Ar (solid line) and N_2–C_2H_2–He (broken line) mixtures.

Petitjean et al. [29]. They found a good agreement between the rotational temperature and the electrode surface temperature and concluded that the rotational temperature may be applied to determine the electrode temperature in nitrogen reactive plasmas. It seems to be also valid for our system and the rotational/gas temperatures presented here can be considered also as the electrode surface temperature.

The vibrational temperatures of CN and N_2 differed considerably both in dc and 100 kHz discharges. A possible explanation for the difference between these vibrational temperatures is that excited species may be produced through various mechanisms. The excited states of CN may be originated from impact of high energy species, e.g. nitrogen with hydrocarbons [16], while the excited states of N_2 may be mainly populated as a result of electron impact excitation [13]. The metastable states of argon, helium as well as nitrogen may also contribute in the production of vibrational excited states of CN and N_2 as reported in literature [13,30]. In the mixture containing argon (N_2–C_2H_2–Ar), the CN vibrational temperature was observed to be higher than that in helium (N_2–C_2H_2–He). It indicates that the energy exchange transfer process from Ar metastable states or other high energy states of Ar to the CN molecule is meaningful. The difference between the CN and N_2 vibrational temperatures (e.g. in the presence of argon and helium) can be treated as an evidence for complex an multichannel process existing in plasma which properties play important role in production and deposition of the CN:H layers.

The different plasma temperature in the mixtures with Ar and He can be associated with such factors as different electron

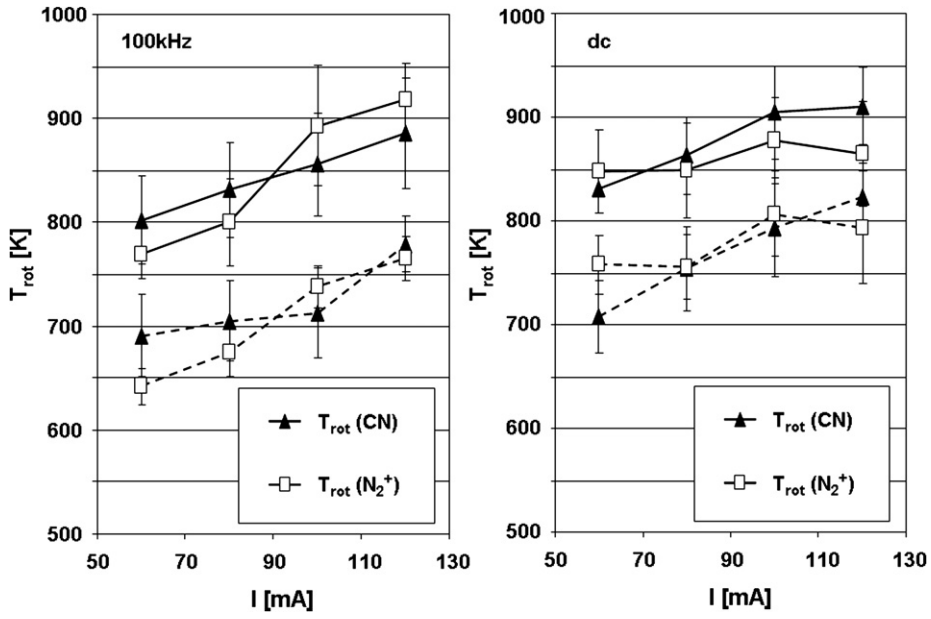

Fig. 8. The CN and N_2^+ rotational temperatures in the N_2–C_2H_2–Ar (solid line) and N_2–C_2H_2–He (broken line) mixtures.

densities in these mixtures, various thermal conductivities of argon and helium, discrepancies in deviation from thermal equilibrium.

In the N_2–C_2H_2–Ar mixture the excitation temperatures of Ar and H were nearly equal, while in the N_2–C_2H_2–He mixture, the He temperature was clearly lower than the H excitation temperature. The addition of argon, instead of helium, to the nitrogen–acetylene mixture caused the growth of the vibrational temperature of CN as well as rotational temperatures. In the nitrogen–acetylene–argon mixture the excitation temperatures of Ar and H were about ten times higher than the rotational temperatures and two times higher than vibrational temperature of CN. The relations between the measured temperatures is as follows:

$$T_{exc}(ArI) > T_{exc}(H) > T_{vib}(CN) > T_{vib}(N_2) > T_{rot}(CN) = T_{rot}(N_2^+)$$

In the nitrogen–acetylene–helium dc and 100 kHz plasmas, the calculated temperatures were differed considerably:

$$T_{exc}(H) > T_{vib}(CN) > T_{exc}(HeI) \geq T_{vib}(N_2) > T_{rot}(CN) = T_{rot}(N_2^+)$$

The significant differences between temperatures (excitation, vibrational, rotational) are evidence that the analyzed plasmas are in the non-equlibrium states.

4. Conclusion

The study of the dc and 100 kHz discharges in the reactive mixtures, i.e. nitrogen–acetylene–argon and nitrogen–acetylene–helium, indicated differences in the processes occurring in these plasmas. The addition of helium to the acetylene–nitrogen mixture caused a growth in the emission intensity of N_2^+, while the addition of argon increased the emission intensities of H, CH and CN independently from the current frequency. The discharge current significantly affected the emission intensities of the CN, C, CH, H, Ar, He, Ar^+ and N_2^+ species.

The distribution of populations of the analyzed excitation, the vibrational and rotational levels were found to follow the Boltzmann's law. An agreement was found between the rotational temperatures derived from N_2^+ and the CN spectra in the dc and the 100 kHz discharges. However, the meaningful differences in the temperatures (excitation, vibrational, rotational) revealed some high deviations of the analyzed plasmas from the thermodynamic equilibrium.

The vibrational temperature of CN as well as the rotational temperature of CN and N_2^+ were sensitive to the changes in the plasma gas composition and the current. The replacement of helium by argon led to an increase in the CN and N_2^+ rotational temperatures and the CN vibrational temperature.

References

[1]. Liu D, Zhou J, Fisher ER. Correlation of gas-phase composition and film properties in the plasma-enhanced chemical vapor deposition of hydrogenated amorphous carbon nitride films. J Appl Phys 2007;101:023304.

[2] Barbadillo L, Hernandez MJ, Cervera M, Piqueras J. Amorphous CNx layers from neon electron cyclotron resonance plasmas with N_2 and CH_4 as precursor. J Electrochem Soc 2000;147:3864.

[3] Camero M, Gordillo-Vazquez FJ, Ortiz J, Gomez-Aleixandre C. Influence of the power on the processes controlling the formation of ECR-CVD carbon nitride films from $CH_4/Ar/N_2$ plasmas. Plasma Sources Sci Technol 2004;13:121.

[4] Gruger H, Selbmann D, Wolf E, Leonhardt A. Deposition of CNx thin films by plasma-activated chemical vapour deposition using various precursors as carbon source. J Mater Sci 1997;32:2847.

[5] Dorner-Reisela A, Kubler L, Irmer G, Reisel G, Schfps S, Klemm V, et al. Characterisation of nitrogen modified diamond-like carbon films deposited by radio-frequency plasma enhanced chemical vapour deposition. Diam Relat Mater 2005;14:1073.

[6] Zhang M, Nakayama Y, Miyazaki T, Kume M. Growth of amorphous hydrogenated carbon nitride films in radio-frequency plasma. J Appl Phys 1999;85:2904.

[7] Clay KJ, Speakman SP, Amaratunga GAJ, Silva SRP. Characterization of a-C:H:N deposition from CH_4/N_2 rf plasmas using optical emission spectroscopy. J Appl Phys 1996;79:7227.

[8] Bhattacharyya S, Vallée C, Cardinaud C, Turban G. Structure of nitrogenated carbon films prepared from acetylene and nitrogen mixture in electron cyclotron resonance plasma. J Appl Phys 2000;87:7524.

[9] Aryal HR, Adhikari S, Ghimire DCh, Uchida H, Umeno M. Argon gas dilution effect on the properties of amorphous carbon nitride thin films. Diam Relat Mater 2007;16:1269.

[10] Kyziol K, Jones S, Tkacz-Smiech K, Marszalek K. A role of parameters in RF PACVD technology of a-C:N:H layers. Vacuum 2008;82:998.

[11] Liu XW, Chan LH, Hsieh WJ, Lin JH, Shih HC. The effect of argon on the electron field emission properties of α-C:N thin films. Carbon 2003;41:1143.

[12] Sung SL, Tseng CH, Chiang FK, Guo XJ, Liu XW, Shih HC. Novel approach to the formation of amorphous carbon nitride film on silicon by ECR-CVD. Thin Solid Films 1999;340:169.

[13] Naveed MA, Rehman NU, Zeb S, Hussain S, Zakaullah M. Langmuir probe and spectroscopic studies of RF generated helium–nitrogen mixture plasma. Eur Phys J D 2008;47:395.

[14] Jamroz P, Zyrnicki W. A spectroscopic study into the decomposition process of titanium isopropoxide in the nitrogen-hydrogen 100 kHz low-pressure plasma. Vacuum 2008;82:651.

[15] Cvelbar U, Krstulovic N, Milosevic S, Mozetic M. Inductively coupled RF oxygen plasma characterization by optical emission spectroscopy. Vacuum 2007;82:224.

[16] Jamroz P, Zyrnicki W. Study of the dc and 100 kHz glow discharges in acetylene–nitrogen mixture by means of optical emission spectroscopy. Eur Phys J Appl Phys 2002;19:201.

[17] Bardos L, Barankova H, Welzel Th, Dani I, Peter S, Richter F. Comparison of the radio frequency hollow cathode to the microwave antenna discharge for plasma processing. J Appl Phys 2001;90:1703.

[18] Okada A, Kijima K. Analysis of optical emission spectra from ICP of Ar–SiH_4–CH_4 system. Vacuum 2002;65:319.

[19] Jamroz P, Zyrnicki W. Spectroscopic study of the decomposition process of tetramethylsilane in the N_2–H_2 and N_2–Ar low pressure plasma. Diam Relat Mater 2005;14:1498.

[20] Durrant SF, de Moraes MAB, Rouxinol FP. Gas-phase and plasma-surface reactions in radiofrequency discharges of C_2H_2–N_2-noble gas mixtures. Thin Solid Films 2001;398–399:156.

[21] Durrant SF, Marcal N, Castro SG, Vinhas RCG, de Moraes MAB, Nicola JH. Mechanisms of polymer film deposition from rf discharges of acetylene, nitrogen and helium mixtures. Thin Solid Films 1995;259:139.

[22] Dinescu G, de Graaf A, Aldea E, van de Sanden MCM. Investigation of processes in low-pressure expanding thermal plasmas used for carbon nitride deposition: I. $Ar/N_2/C_2H_2$ plasma. Plasma Sources Sci Technol 2001;10:513.

[23] Gordillo-Vazquez FJ, Albella JM. Influence of the pressure and power on the non-equilibrium plasma chemistry of C_2, C_2H, C_2H_2, CH_3 and CH_4 affecting the synthesis of nanodiamond thin films from C_2H_2(1%)/H_2/Ar-rich plasmas. Plasma Sources Sci Technol 2004;13:50.

[24] Pereira J, Massereau-Guilbaud V, Geraud-Grenier I, Plain A. CH and CN radical contribution in the particle formation generated in a radio-frequency CH_4/N_2 plasma. Plasma Process Polym 2005;2:633.

[25] NIST atomic spectra database, http://physics.nist.gov/PhysRefData/ASD/index.html.

[26] Jonkers J, van der Mullen JAM. The excitation temperature in (helium) plasmas. J Quant Spectrosc Radiat Transf 1999;61:703.

[27] Kutasi K, Donko Z, Mohai M, Nemes L, Marosi G. Formation of CNx layers in a nitrogen glow discharge with graphite electrodes. Vacuum 2002;68:311.

[28] Shimada M, Tynan GR, Cattolica R. Rotational and translational temperature equilibrium in an inductively coupled plasma. J Vac Sci Technol A 2006;24:1878.

[29] Petitjean L, Ricard A. Emission spectroscopy study of N2–H2 glow discharge for metal surface nitriding. J Phys D Appl Phys 1984;17:919.

[30] Kanda K, Igari N, Kikuchi Y, Kishida N, Igarashi J, Katsumata S, et al. Formation of $CN(B^2\Sigma^+)$ in the reaction of excited argon metastable atoms with some simple nitriles. J Phys Chem 1995;99:5269.